DOI: 10.1002/ejic.201001345

Strategies for Optimizing the Performance of Cyclometalated Ruthenium Sensitizers for Dye-Sensitized Solar Cells

Paolo G. Bomben,[a] Kim D. Thériault,[a] and Curtis P. Berlinguette*[a]

Keywords: Ruthenium / Electrochemistry / Dyes / Sensitizers / Solar cells

Pursuant to our goal of optimizing the performance of cyclometalated Ru sensitizers in the dye-sensitized solar cell (DSSC), the physicochemical properties of a series of tris-heteroleptic Ru^{II} complexes are reported. Each of these complexes contains a metal ligated by: (i) a bidentate 2,2′-bipyridine-4,4′-dicarboxylic acid (dcbpy) ligand to anchor the dye to the TiO_2 surface; (ii) a cyclometalating ligand – with electron-withdrawing groups to ensure a sufficiently high oxidation potential for dye regeneration in the DSSC; and (iii) a 2,2′-bipyridine (bpy) ligand. UV/Vis and electrochemical data reveal that each complex exhibits broad metal-to-ligand charge transfer (MLCT) bands of significant intensity ($\varepsilon = 1.0–2.3 \times 10^4\ M^{-1}\,cm^{-1}$) in the visible region, and ground- and excited-state redox potentials that are appropriate for sensitizing TiO_2. Analysis of the dyes in the DSSC highlights the sensitivity of cell performance to the oxidation potential for each of the dyes, which has important implications in the development of cyclometalated Ru sensitizers.

Introduction

The relatively low embodied energy of the dye-sensitized solar cell (DSSC) makes this technology a promising alternative to conventional solar cell materials – particularly for smaller scale applications that rely on nonideal light conditions.[1–4] Although the DSSC currently stands out as the most efficient third-generation solar cell technology,[5] there remains the need to further improve the power conversion efficiency (η) of these cells beyond the current benchmark of 12.1%.[6] While a growing body of research has been directed at improving the anode material (e.g., TiO_2,[7] ZnO[8]) and the electrolyte [e.g., I^-/I_3^-,[9] Ni^{III}/Ni^{IV} bis(dicarbollide),[10,11] polythiophene[12]], our program has joined the broad effort to expand the catalogue of light harvesting molecules in pursuit of robust and high performance devices.[13–15]

Pioneering DSSC studies by Grätzel et al., utilized the dye complex, $Ru(dcbpy)_2(NCS)_2$ (**N3**), to generate efficiencies greater than 10%.[16,17] Since that discovery, the limited set of *bona fide* champion (i.e., $\eta > 10\%$) dyes that have emerged in the literature bear many of the same structural elements as **N3**.[1,6,17–26] There are, however, some notable recent findings that outline alternative approaches to dye design. Examples include the recent report of the first champion *organic* dye by Wang et al.,[27] and the remarkably high efficiency of a porphyrinatozinc derivative by Diau et al.[28] Another important development directly relevant to this study is the recognition that Ru dyes devoid of NCS^- ligands are capable of achieving efficiencies that approach or exceed 10%.[29,30] These findings provide the imperative to further the development of cyclometalated Ru^{II} derivatives[31–38] in the context of the DSSC.[39–41]

Cyclometalated Ru complexes of type $[Ru^{II}(N^{\wedge}N)_2(C^{\wedge}N)]^z$ [$N^{\wedge}N$ = dcbpy (2,2′-bipyridine-4,4′-dicarboxylic acid); $C^{\wedge}N$ = bidentate cyclometalating ligand; e.g., ppy (2-phenylpyridine); z = 0 or +1] are generally characterized by a highest occupied molecular orbital (HOMO) that is predominantly metal-based, but with orbital character extended to the anionic ring of the cyclometalating ligand.[40,42] The orbital character of the low-lying excited states resides on the π* framework of the $N^{\wedge}N$ ligands (e.g., anchoring dcbpy ligands); the π*-system of the $C^{\wedge}N$ ligand often lies higher in energy by ca. 1.2 eV. The increased donor strength of the $C^{\wedge}N$ ligands raises the energy of the metal *d*-orbitals resulting in a complex that is easier to oxidize; e.g., E_{ox} = +0.70 and +1.52 V vs. NHE (MeCN) for $[Ru(bpy)_2(ppy)]^+$ and $[Ru(bpy)_3]^{2+}$, respectively.[40] The ligand π*-systems are also shifted to higher energies, but to a lesser extent, which leads to a bathochromic shift of the lowest-energy UV/Vis absorption bands. The lower molecular symmetry lowers the degeneracy of the energy levels to produce a series of *broad* absorbance bands.

An important observation is that the perturbation of the $C^{\wedge}N$ ligand-field renders a HOMO analogous to the paradigmatic **N3** complex with respect to the orbital character being delocalized over the metal *and* anionic ligand(s). Unlike **N3**, however, $C^{\wedge}N$ ligands provide the opportunity for further chemistry because the HOMO level can be easily modulated through the judicious installation of terminal

[a] Department of Chemistry University of Calgary,
2500 University Drive NW, Calgary, Alberta, T2N 1N4, Canada
Fax: +1-403-289-9488
E-mail: cberling@ucalgary.ca

Supporting information for this article is available on the WWW under http://dx.doi.org/10.1002/ejic.201001345.

substituents.[42] This feature provides a significant amount of leverage for optimizing the numerous factors that must be in alignment for efficient sensitization (e.g., appropriate ground- and excited-state redox properties, high molar extinction coefficients, appropriate electron-transfer kinetics).[13,43]

A strategy that has proven to be effective for conventional dyes is the use of a *tris*-heteroleptic ligand environment; indeed, the significant majority of champion dyes are variations of **N3**, where one dcbpy ligand has been replaced with a bpy ligand bearing bulky, conjugated substituents.[1,6,20–26] These substituents can be used to absorb more light *and* suppress recombination processes between the electrolyte and the TiO_2. Moreover, the use of hydrophobic chains can lend stability to the device by inhibiting water from reaching the surface and affecting the interaction with the anchoring group.[23,26,44]

The objective of this study is to combine said design strategies to develop a series of tris-heteroleptic cyclometalated Ru^{II} complexes for the purpose of sensitizing TiO_2 in the DSSC. There is currently no example of such a *C^N* complex in the literature that is poised for sensitizing TiO_2; indeed, to the best of our knowledge, the only literature precedent for a *tris*-heteroleptic cyclometalated Ru^{II} complex is [Ru(bpy)(5,6-Me_2phen)(ppy)](PF_6) (5,6-Me_2phen = 5,6-dimethyl-1,10-phenanthroline) reported by Ryabov et al.[45] To fill this void in the literature, we outline herein a series of complexes broadly formulated as [Ru(bpy)(dcbpy)(*C^N*)]$^+$ (**1d**–**3d**, Scheme 1). Each complex contains: (i) a dcbpy ligand to anchor the dye to the TiO_2; (ii) an unsubstituted bpy ligand; and (iii) a cyclometalating ligand with various terminal substituents. The substituents were selected by virtue of their electron-withdrawing character to ensure a thermodynamic driving force exists for dye regeneration (e.g., 200, 430, and 230 mV for **1d**–**3d**, respectively, where $E_{1/2}$ (I^-/I_3^-) ≈ +0.5 V vs. NHE); the thiophene-aldehyde substituent was utilized to expand the orbital character of the HOMO to further improve the light-harvesting capacity of the complex (the aldehyde serves to increase E_{ox}).[42] While the bpy ligand does not contain bulky substituents, it serves as a placeholder for such ligands in future studies. A comparative cell performance is reported to underscore the need for sufficiently high oxidation potentials to achieve optimal power output. This article provides a proof-of-concept for the application of these dyes in the DSSC, and outlines important guiding principles for further improving the performance of this class of sensitizers.

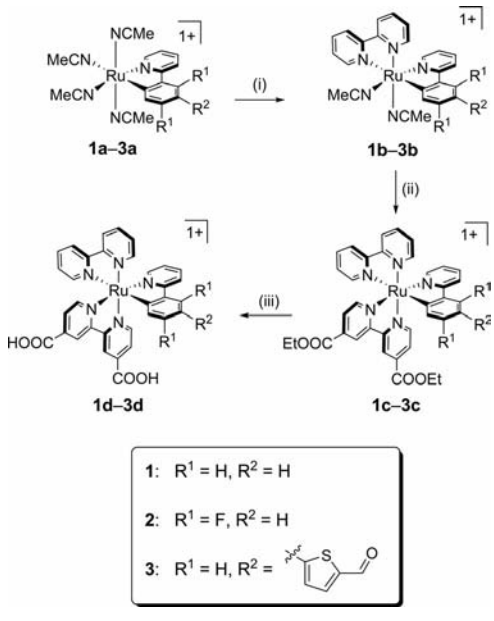

Scheme 1. Synthetic protocol for tris-heteroleptic ruthenium sensitizers: (i) bpy, CH_2Cl_2, room temp., 20 h (**1a**, **3a**); bpy, CH_2Cl_2, reflux, 20 h (**2a**); (ii) deeb, EtOH, reflux, 3 h; (iii) 3:1:1 DMF/H_2O/NEt_3, reflux, 16 h. Counteranion is PF_6^- for all complexes.

Results and Discussion

Synthesis and Characterization

To the best of our knowledge, the only documented example of a tris-heteroleptic cyclometalated Ru^{II} complex is [Ru(bpy)(5,6-Me_2phen)(ppy)](PF_6).[45] Synthetic access to this complex is provided by the synthon, [Ru(CH_3CN)$_4$(ppy)](PF_6) (**1a**), which is amenable to subsequent reactions with bpy and 5,6-Me_2phen under moderate reaction conditions (e.g., 60–65 °C, MeOH). This facile synthetic pathway does not, however, fully translate to our target complexes because of the electron-*withdrawing* substituents on the *C^N* and polypyridyl ligands; moreover, the presence of –CO_2H anchoring groups on DSSC dyes is not generally compatible with syntheses in purely organic solvents. Consequently, the preparative route described above had to be modulated to accommodate these structural and electronic disparities.

We have shown in prior work that [Ru(CH_3CN)$_4$(*C^N*)](PF_6) and [Ru(CH_3CN)$_2$(*p*-cymene)(*C^N*)](PF_6) are suitable synthons for subsequent reactions with bpy derivatives.[42] While both precursors form in approximately equimolar concentrations under our reaction conditions, they were shown to converge on the same product {e.g., [Ru(dcbpy)$_2$(*C^N*)]$^+$} during the subsequent ligation step. Our efforts to isolate **1b** using this same protocol (in a refluxing CH_2Cl_2 medium) resulted in a mixture of [Ru(CH_3CN)$_2$(bpy)(ppy)](PF_6) and [Ru(bpy)$_2$(ppy)](PF_6), as well as [Ru(CH_3CN)$_2$(*p*-cymene)(ppy)](PF_6). Because the latter species does not react with bpy (or dcbpy) to an appreciable extent, the precursor [Ru(CH_3CN)$_4$(*C^N*)](PF_6) is a critical starting point for our syntheses. The reagent [Ru(C_6H_6)Cl_2]$_2$ furnishes the desired precursor in exclusivity according to the method described by Pfeffer et al.[35]

The subsequent reaction step to form **1b** is relatively facile (Scheme 1); i.e., all of the bpy is consumed during the formation of **1b** within 20 h at ambient temperatures {a minor quantity of the [Ru(bpy)$_2$(ppy)](PF_6) byproduct is formed}. This procedure was less successful in the case of **2b**: less than 10% of the bpy starting material was consumed over 20 h. Our interpretation of this result is that the electron-withdrawing nature of the ppy-F_2 ligand dimin-

ishes the electron density at the Ru^{II} centre, thereby suppressing the displacement of the CH_3CN donor ligand by bpy at ambient temperatures. Elevated reaction temperatures (e.g., 35 °C) do help drive the consumption of bpy, but this procedure results in a ca. 70:30 mixture of $[Ru(CH_3CN)_2(bpy)(ppy\text{-}F_2)](PF_6)$/$[Ru(bpy)_2(ppy\text{-}F_2)](PF_6)$, along with residual $[Ru(CH_3CN)_4(ppy\text{-}F_2)](PF_6)$. Further complications were encountered during purification: **2b** reverts to **2a** during the column chromatography separation steps. These challenges were not observed in the case of **3b**, which could be isolated using the same method as **1b**. The outcome of these reactions highlights how electronic parameters affect the loss of the MeCN ligand; namely, an electron-deficient Ru metal centre inhibits the displacement of MeCN at ambient temperatures.

We note that the addition of diethyl 2,2′-bipyridine-4,4′-dicarboxylate (deeb) to **1a**–**3a** prior to the addition of bpy results in the formation of $[Ru(deeb)_2(C\text{^}N)](PF_6)$ as the major product. We attribute this result to a stronger synergistic bonding interaction with Ru, which effectively stabilizes the low-lying π* orbitals to a greater extent than bpy. On this basis, the last ligand binding step was reserved for the deeb ligand.

Addition of deeb to **1b**–**3b** to form **1c**–**3c** occurs quantitatively in refluxing EtOH over 2–3 h. The use of other low-boiling, non-coordinating solvents (e.g., $CHCl_3$ or MeOH) resulted in lower yields and purity. We were unable to obtain **3c** in sufficient purity despite numerous attempts to separate it from residual deeb by column chromatography; however, the hydrolyzed sensitizer **3d** could be separated and isolated in sufficient purity using SiO_2 and Sephadex. The conversion to acid complexes **1d**–**3d** results in a small amount of ligand scrambling; e.g., $[Ru(dcbpy)_2(C\text{^}N)](PF_6)$ and $[Ru(bpy)_2(C\text{^}N)](PF_6)$ both form as minor byproducts. The separation of these byproducts from the target complexes **1d**–**3d** was complicated by the high solubility of all three species after hydrolysis, and creates a more challenging purification process than with the tridentate analogues.[41] Purification of all acid complexes required column chromatographic techniques. Complexes **1d** and **3d** exist as a 1:1 equilibrium mixture containing fully protonated and singly protonated dcbpy ligands, while **2d** exists in a 1:3 fully/singly protonated mixture.

This difference is rationalized by the electron-rich nature of **1d** and **3d** disabling the stabilization of the negative charge on the peripheral dcbpy ligand. Conversely, **2d** is better able to compensate the negative charge to stabilize the deprotonated form. Our efforts to verify this feature by NMR spectroscopy were not successful due to solubility issues in aprotic apolar solvents. These diacid complexes, similar to their tetraacid analogues,[42] were found to be hygroscopic (i.e. up to four water molecules per sensitizer); extended periods under vacuum did not remove this water.

All of the metal complexes **1a**–**3d** were characterized by ^1H NMR spectroscopy, mass spectrometry and elemental analysis. The chemical shift of the proton *ortho* to the organometallic bond is a useful spectroscopic handle for identifying the formation of the title complexes because it resides as the most upfield signal in the aromatic region.[34,40,42,47] This scenario was found to hold true for **1c**–**3c** and **1d**–**3d**, but not in the cases of **1b**–**3b**, where this same signal resides ca. 1.8 ppm downfield (δ = 8.20–8.37 ppm; see Figure S1 in the Supporting Information). The upfield location in **1c**–**3c** and **1d**–**3d** is a consequence of the *ortho* proton being shielded by an adjacent pyridine ring that is not present in **1b**–**3b**. The bpy proton directed at the MeCN ligand represents another diagnostic signal for **1b**–**3b**; this proton resonance occurs at ca. 9.4 ppm.

Electrochemical Properties

The electrochemical behavior of all of the isolated complexes in Figure 1 was examined by cyclic voltammetry. Relevant redox potentials in DMF are presented in Table 1; representative voltammograms are presented for **1a**–**1d** in Figure S2.

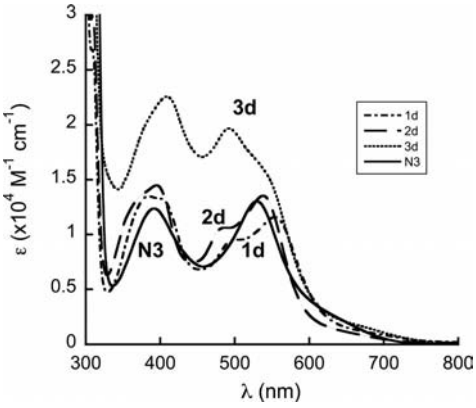

Figure 1. UV/Vis spectra of methanolic solutions of **1d**–**3d**. The spectrum for **N3** is included as a benchmark.

The cyclic voltammograms for **1c** and **2c**, each of which contain three bidentate ligands, reveal two reversible reduction waves and a single oxidation wave. The first reduction wave, E_{red1}, of **1c** is shifted to more positive potentials by ca. +450 mV relative to **1b**; this reversible wave is assigned to the π* manifold of the deeb ligand. The second reversible reduction wave, E_{red2}, at –1.39 V is assigned to the reduction of the bpy ligand. The redox behavior of **2c** follows the expected trends given the electron-withdrawing character of the –F groups: all of the redox waves are observed at higher potentials relative to **1c**, the E_{ox1} value being affected to the greatest extent.

The corresponding acid species, **1d**–**2d**, each display a lower oxidation potential relative to **1c**–**2c**. The magnitude of this effect is greater for **1** ($\Delta E_{1/2}$ = 140 mV) than **2** ($\Delta E_{1/2}$ = 60 mV) because of the diminished electron density at the metal center arising from the –F groups. The 2-thiophene-5-carbaldehyde moiety on the ppy ligand shifts the E_{ox1} value only +30 mV relative to **1d**, while the two –F groups raise this potential by over +200 mV. A single reductive wave assigned to the reduction of dcbpy is observed for each of the three acid complexes, and displays only a minor sensitivity to substituents on the ppy ligand (E_{red1} =

Table 1. Spectroelectrochemical data.

Compound[a]	UV/Vis data[b]			Emission data		$E_{1/2}$ (V vs. NHE)	
	λ_{max1} [nm]	λ_{max2} [nm]	λ_{max3} [nm]	λ_{em} [nm][c]	τ [ns][d]	E_{ox1}	E_{red1}
$[Ru(CH_3CN)_2(bpy)(ppy)]^+$ (**1b**)	371 (0.90)	488 (0.61)	–	735 (488)	10.7 (1.10)	+0.83[e]	–1.35[e]
$[Ru(CH_3CN)_2(bpy)(ppy4thio)]^+$ (**3b**)	403 (1.7)	477 (sh)	–	723 (477)	9.7 (1.20)	+0.87[f]	–1.34[f]
$[Ru(deeb)(bpy)(ppy)]^+$ (**1c**)	421 (1.2)	498 (0.9)	575 (1.4)	–	–	+0.84[e]	–0.91[e]
$[Ru(deeb)(bpy)(ppy\text{-}F_2)]^+$ (**2c**)	399 (1.4)	482 (1.0)	556 (1.5)	–	–	+0.99[e]	–0.87[e]
$[Ru(dcbpy)(bpy)(ppy)]^+$ (**1d**)	394 (1.3)	503 (1.0)	554 (1.2)	787 (554)	9.3 (1.02)	+0.70[f]	–1.37[f]
$[Ru(dcbpy)(bpy)(ppy\text{-}F_2)]^+$ (**2d**)	395 (1.4)	488 (1.1)	538 (1.4)	761 (538)	27.0 (1.07)	+0.93[f]	–1.35[f]
$[Ru(dcbpy)(bpy)(ppy4thio)]^+$ (**3d**)	409 (2.3)	492 (2.0)	543 (sh)	779 (543)	14.1 (1.05)	+0.73[f]	–1.40[f]

[a] Counteranion is PF_6^- for all complexes. Data for **2b** and **3c** not provided due to purification issues (see Exp. Section for details). [b] Recorded in MeOH; ε values indicated in parentheses with units of $\times 10^4$ M^{-1}cm^{-1}. [c] λ_{ex} indicated in parentheses with units of nm. [d] χ^2 indicated in parentheses. [e] Data collected using 0.1 M NBu_4BF_4 DMF solutions at 200 mV/s and referenced to a $[Fc]/[Fc]^+$ internal standard, followed by conversion to NHE {$[Fc]/[Fc]^+$ vs. NHE = 0.69 V}.[46] [f] Data collected using 0.1 M NBu_4BF_4 DMF solutions at 200 mV/s and referenced to octamethylferrocene (OFc) $[OFc]/[OFc]^+$ internal standard followed by conversion to NHE {$[OFc]/[OFc]^+$ vs. NHE = +0.29 V}.

–1.35 V to –1.40 V). While the excited-state oxidation potentials [$E(S^+/S^*)$: –1.05 (**1d**), –0.91 (**2d**) and –1.10 V vs. NHE (**3d**)] were found to be at least 400 mV higher than the TiO_2 conduction band (assuming E_{cb} = –0.5 V vs. NHE),[48] the relatively low ground-state oxidation potentials for **1d** and **3d**, which are positioned only ca. 250–300 mV lower in energy than the I^-/I_3^- couple, appear to pose a problem for dye regeneration (vide infra).

Electronic Spectroscopy

UV/Vis absorbance spectra were recorded on solutions containing each of the metal complexes; the positions of key absorption maxima in the visible region are listed in Table 1. Broad absorbance bands are observed for each of the complexes arising from a series of mixed-metal/ligand-to-ligand charge-transfer transitions in the visible region, and a suite of intense intraligand π-π* transitions that occur below 330 nm. Although DFT studies show that the HOMO character spans both the metal and anionic ring of the *C^N* ligand, the reversibility of the electrochemical wave indicates that the electron density is situated predominantly on the metal; thus, transitions arising from these mixed orbitals to a ligand are classified herein as metal-to-ligand charge transfer (MLCT) for simplicity.[40,49]

The successive addition of bidentate ligands to the Ru center in complexes **1a**–**1d** presents the opportunity to systematically examine how the absorbance bands are affected by progressive ligation (see Figure S3). The optical data for **1d**–**3d** (Figure 1) reveals how terminal substituents on the *C^N* ligand affect the optical properties. The higher intensity of the MLCT absorbance bands for **3d** relative to **1d** and **2d**, for instance, demonstrates how extending the conjugation away from the metal center with the substituent, 2-thiophene-5-carbaldehyde, is an effective strategy for increasing ε values.[42] This expansion of the HOMO orbital character increases the optical cross section and the transition dipole moment to render a more strongly absorbing complex;[50–52] e.g., integration of the UV/Vis data between 350–800 nm shows that **3d** absorbs 1.7 times more light than **1d**. The blue-shift and lower intensities of λ_{max3} for **1d** and **2d** relative to **1c** and **2c** is ascribed to a shift to higher-energy for the lowest π* energy levels upon conversion from deeb to dcbpy. The lowest-energy absorbance band maxima, λ_{max3}, track the relative positions of the HOMO levels and are found at progressively longer wavelengths for **2d**, **3d** and **1d**, respectively (Figure 1).

While **1d** and **2d** exhibit similar absorption profiles to the paradigmatic **N3** dye in terms of intensity and onset of absorption, the highest light-harvesting capacity among the sensitizers in this study is **3d** (Figure 1). This observation provides a clear indication that the extended conjugation of **3d** increases the entire absorption envelope, thereby lending credence to our approach of installing conjugated substituents on the anionic ring of the *C^N* ligand.

Solar Cell Performance

DSSCs were prepared with **1d**–**3d** using a uniform set of fabrication conditions (e.g., dye-loading concentration, electrolyte solution, TiO_2 film treatment) to establish the relative performance of the sensitizers. Dye loading studies confirmed that each dye has a similar molecular footprint on TiO_2; e.g., surface coverage was measured to be ca. 1×10^{-7} mol/cm^2 for **1d**–**3d**. Because the molecular charge, anchoring ligand (e.g., dcbpy), and ancillary (e.g., bpy) ligand are all held at parity within the series, any significant differences in cell performance can be attributed to substituents on the cyclometalating ligand.

A listing of the corresponding solar cell metrics in Table 2 indicate that cell power conversion efficiencies (η) parallel short-circuit current (J_{sc}); i.e., **2d** (4.02%, 10.79 mA/cm^2) > **3d** (2.45%, 6.72 mA/cm^2) > **1d** (2.39%, 6.34 mA/cm^2) (Figure 2). This trend does not, however, track with the relative light absorption of the complexes (e.g., the cell performance of **3d** is only marginally better than that of **1d** despite absorbing 1.7 times more visible light), thus indicating that other factors dominate cell performance. This point is underscored by the significantly higher J_{sc} value for **2d** in the series, despite the superior absorption manifold for **3d**. IPCE data collected for **1d**–**3d** (Figure S4) confirms this observation with **2d** plateauing at 50% at λ = 548 nm, while **1d** and **3d** exhibit relatively inferior conversion efficiencies throughout the visible spec-

trum, particularly at > 650 nm. Because of the comparable molecular footprints for the dyes, the disparities in J_{sc} for the series is reasoned to be a retardation of electron-transfer processes. We note that the lowest $E(S^+/S^*)$ value is measured for **2d** (–0.91 V vs. NHE) within the series; thus, it is unlikely that the photoreducing capacity of the dye is responsible for the observed trends in cell performance. Assuming that the I^-/I_3^- redox couple is +0.5 V vs. NHE (we caution that this value is reported to range between +0.35 to +0.58 V vs. NHE[29,30,48,53]), there exists a thermodynamic driving force of ca. 430 mV to regenerate **2d**, which is significantly greater than the 200–230 mV for **1d** and **3d**.

Table 2. Cell performance data for **1d**–**5d**.

Dye	V_{oc} [mV]	J_{sc} [mA/cm^2]	*FF* [%]	η [%]	$E_{1/2ox}$(V vs. NHE)
1d	0.592	6.34	63.7	2.39	+0.70
2d	0.597	10.79	61.9	4.02	+0.93
3d	0.595	6.72	60.6	2.45	+0.73
4d[a]	0.633	9.75	61.3	3.82	+1.06
5d[b]	0.610	8.36	64.4	3.30	+0.92 (estimated)
N3	0.743	14.76	62.5	6.92	+1.09

[a] **4d** = $[Ru(dcbpy)_2(ppy\text{-}F_2)][PF_6]$. [b] **5d** = $[Ru(dcbpy)_2(ppy4thio)][PF_6]$.

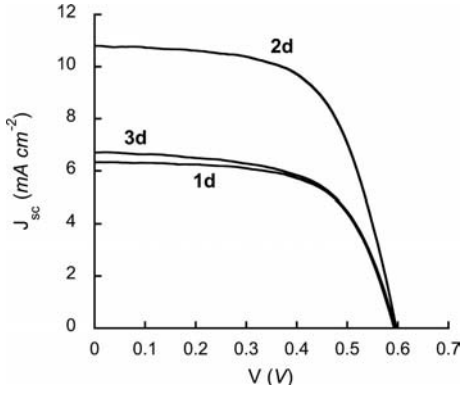

Figure 2. Current-voltage characteristics of cells constructed with dyes **1d**, **2d** and **3d**.

It has been reported that a minimum of 150 mV is required for dye regeneration to occur,[54,55] thus, the E_{ox1} values for **1d** and **3d** should, in principle, be sufficient for dye regeneration. A careful perusal of the literature, however, reveals that all of the Ru-based champion dyes have E_{ox1} values greater than +0.85 V vs. NHE.[1,6,17–26] Taking this observation into account, we ascribe the relatively inferior performance of devices sensitized by **1d** and **3d** to be a consequence of insufficient driving force of regeneration by the electrolyte, despite the superior absorption profile of **3d**. This observation has significant implications for further developing this new class of sensitizers: optimal cell performance will require sufficiently strong electron-withdrawing groups on the *C^N* ligands to offset the replacement of dcbpy with a bpy derivatized with alkyl/conjugated substituents.

Complexes **4d** and **5d** from our previous studies were measured under the same cell conditions as **1d**–**3d** to examine how the number of anchoring groups affects performance (we note that 1 equiv. of Bu_4NOH was required to dissolve **4d** and **5d** in ABS EtOH). The larger η for **4d** relative to **5d** is rooted in the higher V_{oc} and J_{sc} values. The relative J_{sc} values are again attributed to a consequence of a higher oxidation potential for **4d** (+1.06 V vs. NHE) compared to **5d** (ca. +0.92 V vs. NHE). The improved V_{oc} may be manifest in the different molecular dipoles of the dyes (e.g., **4d** = 8.0 Debye (D); **5d** = 16.5 D[56]) affecting the conducting band (E_{cb}) of the TiO_2;[57,58] more comprehensive studies are underway to verify this effect. Cells constructed from the tetraacid complexes **4d** and **5d** exhibit slightly larger V_{oc} values than the tris-heteroleptic analogues **2d** and **3d**. While this result could be ascribed to a number of factors (e.g., variable amounts of Bu_4N^+ affect the shielding of the TiO_2 surface,[59] the higher oxidation potentials of the dyes affecting the redox couple of the electrolyte), it is consistent with previous findings that have shown binding through a single dcbpy unit results in a lower V_{oc} compared to dyes containing two dcbpy ligands.[57] Electrochemical impedance measurements confirm a smaller interfacial resistance exists between TiO_2 and the electrolyte for **2d** (20 Ω) compared to **4d** (30 Ω). Work is underway to systematically improve each of these processes within these devices.

Conclusions

A series of tris-heteroleptic cyclometalated ruthenium(II) complexes were examined in the context of the development of dye-sensitized solar cells. It was shown that power conversion efficiencies (η) range from 2.39–4.02% for the series **1d**–**3d**. The relative performance of these dyes is dominated by the oxidation potential of the metal complex: ground-state oxidation potentials of ca. +0.70 V vs. NHE do not appear to be sufficient for effective dye regeneration; better performance was achieved with dyes exhibiting higher E_{ox1} values (e.g., > +0.85 V vs. NHE for **2d**). While extending the conjugation on the anionic donor (e.g., **3d**) was found to improve light absorption by about 1.7-fold within the series, overall cell performance was compromised by the insufficiently high E_{ox1} values. This rationale is corroborated by the fact that the majority of champion dyes are characterized by E_{ox1} values that are higher than +0.85 V vs. NHE.[1,6,17–26] This finding calls attention to the fact that cyclometalated Ru^{II} DSSC chromophores with three unique ligands will require appropriately positioned electron-withdrawing substituents if commercially relevant DSSC performance parameters are to be reached.

Experimental Section

Preparation of Compounds: All manipulations were performed using solvents passed through an MBraun solvent purification system prior to use; chloroform ($CHCl_3$) and tetrahydrofuran (THF)

solvents were analytical grade (without stabilizer). All reagents were purchased from Aldrich unless otherwise stated. 2-phenylpyridine (ppy), 2-(2,4-difluorophenyl)pyridine (ppy-F_2) and 2,2′-bipyridine (bpy) were used as supplied from Aldrich. $[Ru(C_6H_6)Cl_2]_2$,[60] 5-[3-(pyridin-2-yl)phenyl]thiophene-2-carbaldehyde (ppy4thio),[42] diethyl 2,2′-bipyridine-4,4′-dicarboxylate (deeb),[61] 2,2′-bipyridine-4,4′-dicarboxylic acid (dcbpy),[61] complexes **1a**,[35] **1b**,[62] **4d**,[42] **5d**[42] and **6d**[42] were prepared as previously reported. Purification by column chromatography was carried out using silica (Silicycle: Ultrapure Flash Silica), and basic alumina (Fluka). Analytical thin-layer chromatography (TLC) was performed on aluminum-backed sheets pre-coated with silica 60 F254 adsorbent (0.25 mm thick; Merck, Germany) or with plastic-backed sheets pre-coated with basic alumina 200 F254 adsorbent (0.25 mm thick, Selecto Scientific: Georgia, USA) and visualized under UV light. ^{1}H NMR chemical shifts (δ) are reported in parts per million (ppm) from low to high field and referenced to residual non-deuterated solvent. Standard abbreviations indicating multiplicity are used as follows: s = singlet; d = doublet; t = triplet; m = multiplet. General labeling scheme for ^{1}H NMR assignments for all compounds follows Figure S1 in the Supporting Information. Elemental analysis (EA), electrospray ionization (ESI), matrix-assisted laser desorption/ionization time of flight (MALDI-TOF), and electron impact (EI) mass spectrometry (ES) data were collected at the University of Calgary.

$[Ru(CH_3CN)_4(ppy)](PF_6)$ (1a): Synthesized as previously reported. All characterization data matches that previously reported. UV/Vis: λ_{max1} = 377 nm (0.59×10^4 M^{-1} cm^{-1}), λ_{max2} = 436 (sh). Electrochemistry: E_{ox1} = +0.73 V vs. NHE.

$[Ru(CH_3CN)_4(ppy\text{-}F_2)](PF_6)$ (2a): To a flask containing $[Ru(C_6H_6)Cl_2]_2$ (295 mg, 0.589 mmol), NaOH (47 mg, 1.2 mmol) and KPF_6 (434 mg, 2.36 mmol) was added degassed MeCN (10 mL). A solution of ppy-F_2 (0.18 mL, 1.2 mmol) was added to the reaction mixture via syringe, and then heated at 45 °C for 20 h. The solution was filtered and then purified by column chromatography [Al_2O_3 (basic): CH_2Cl_2/MeCN, 9:1]. The first yellow band was isolated and then reconstituted in CH_2Cl_2. A yellow solid product (624 mg, 88.1%) was drawn out of solution by the slow addition of diethyl ether. ^{1}H NMR (CD_3CN): δ = 8.97 (ddd, ^3J = 5.7, ^4J = 1.7, ^5J = 0.8 Hz, 1 H, H_h), 8.14 (d, ^3J = 8.2 Hz, 1 H, H_e), 7.78 (m, 1 H, H_f), 7.52 (dd, $^3J_{HF}$ = 8.7, ^4J = 2.4 Hz, 1 H, H_a), 7.20 (ddd, ^3J = 7.2, 5.7, ^4J = 1.4 Hz, 1 H, H_g), 6.48 (ddd, $^3J_{HF}$ = 13.0, 8.7, ^4J = 2.4 Hz, 1 H, H_c), 2.52 (s, 3 H), 2.02 (s, 6 H), 1.96 (s, 3 H) ppm. MS (ESI): m/z = 414.8 [M^+ – CH_3CN] (calcd. for $[RuC_{17}H_{15}F_2N_4]^+$: m/z = 415.0). $RuC_{19}H_{18}N_5PF_8$ (600.41): calcd. C 38.01, H 3.02, N 11.66; found C 37.98, H 2.97, N 11.27. UV/Vis: λ_{max1} = 383 nm (0.53×10^4 M^{-1} cm^{-1}), λ_{max2} = 430 (sh). Electrochemistry: E_{ox1} = +0.94 V vs. NHE.

$[Ru(CH_3CN)_4(ppy4thio)](PF_6)$ (3a): To a flask containing $[Ru(C_6H_6)Cl_2]_2$ (176 mg, 0.352 mmol), NaOH (28 mg, 0.70 mmol) and KPF_6 (258 mg, 1.40 mmol) was added ppy4thio (4.44 mL, 42.0 mg/mL solution in MeCN) via syringe. The reaction was heated at 45 °C for 45 h, then filtered and purified by column chromatography [Al_2O_3 (basic): CH_2Cl_2/MeCN, 9:1]. The first yellow band was isolated, reconstituted in CH_2Cl_2, then drawn out of solution with diethyl ether to yield 308 mg (64.8%) of the product as a brown solid. ^{1}H NMR (CD_3CN): δ = 9.86 (s, 1 H, H_y), 8.94 (ddd, ^3J = 5.7, ^4J = 1.6, ^5J = 0.7 Hz, 1 H, H_h), 8.12 (d, ^3J = 7.9 Hz, 1 H, H_a), 8.07 (d, ^3J = 8.0 Hz, 1 H, H_e), 8.07 (d, ^4J = 2.0 Hz, 1 H, H_d), 7.87 (d, ^3J = 4.0 Hz, 1 H, H_w), 7.81 (ddd, ^3J = 9.0, 7.4, ^4J = 1.6 Hz, 1 H, H_f), 7.61 (d, ^3J = 4.0 Hz, 1 H, H_x), 7.46 (dd, ^3J = 7.9, ^4J = 2.0 Hz, 1 H, H_b), 7.23 (ddd, ^3J = 7.3, 5.7, ^4J = 1.4 Hz, 1 H, H_g), 2.53 (s, 3 H, $H_{a'}$), 2.01 (s, 6 H, $H_{b',c'}$), 1.96 (s, 3 H) ppm. MS (ESI): m/z = 407.0 [M^+ – 3 CH_3CN] (calcd. for $[RuC_{18}H_{13}N_2SO]^+$: m/z = 407.0). $RuC_{24}H_{22}N_5OSPF_6$ (674.56) + 0.5 CH_2Cl_2 (84.93): calcd. C 41.58, H 3.25, N 9.96; found C 41.63, H 3.24, N 9.71. UV/Vis: λ_{max1} = 411 nm (1.8×10^4 M^{-1} cm^{-1}). $E_{1/2ox}$ = +0.80 V vs. NHE.

$[Ru(bpy)(CH_3CN)_2(ppy\text{-}F_2)](PF_6)$ (2b): A flask containing **2a** (250 mg, 0.416 mmol) and bpy (59.6 mg, 0.382 mmol) in CH_2Cl_2 (50 mL) was heated for 15 h at 35 °C. The dark orange/red solution was passed down a column [Al_2O_3 (basic): CH_2Cl_2, 3 × 1.2 cm; R_f = 0.16] to yield an orange/red solid. The isolated product contains the impurity $[Ru(CH_3CN)_4(ppy\text{-}F_2)][PF_6]$ (10% on a molar basis). The mixture was used as prepared in subsequent reactions because efforts to purify the mixture were unsuccessful.

$[Ru(bpy)(CH_3CN)_2(ppy4thio)](PF_6)$ (3b): A flask containing **3a** (251 mg, 0.372 mmol) and bpy (58.4 mg, 0.374 mmol) in CH_2Cl_2 was stirred for 29 h at ambient temperature. The solvent was then removed under reduced pressure to afford a dark orange/red solid. The crude solid was reconstituted in MeCN/CH_2Cl_2 (1:1), drawn out of solution by layering with Et_2O and filtered to yield a red/brown solid (249 mg, 89.7%). ^{1}H NMR (CD_3OD): δ = 9.86 (s, 1 H, H_y), 9.44 (ddd, ^3J = 5.3, ^4J = 1.5, ^5J = 0.8 Hz, 1 H, H_p), 8.61 (d, ^3J = 8.2 Hz, 1 H, H_m), 8.38 (d, ^3J = 7.9, ^4J = 1, ^5J = 1 Hz, 1 H, H_l), 8.37 (d, ^3J = 7.9 Hz, 1 H, H_a), 8.24 (m, 2 H, $H_{d,n}$), 8.08 (d, ^3J = 8.1 Hz, 1 H, H_e), 7.99 (ddd, ^3J = 5.7, ^4J = 1.5, ^5J = 0.6 Hz, 1 H, H_i), 7.95 (d, ^3J = 4.0 Hz, 1 H, H_x), 7.91 (ddd, ^3J = 7.6, 5.3, ^4J = 1.2 Hz, 1 H, H_o), 7.73 (ddd, ^3J = 8.1, 7.6, ^4J = 1.6 Hz, 1 H, H_k), 7.69 (d, ^3J = 4.0 Hz, 1 H, H_w), 7.63 (ddd, ^3J = 8.1, 7.4, ^4J = 1.2 Hz, 1 H, H_f), 7.63 (dd, ^3J = 7.8, ^4J = 2.0 Hz, 1 H, H_b), 7.49 (ddd, ^3J = 5.7, ^4J = 1.5, ^5J = 0.7 Hz, 1 H, H_h), 7.07 (ddd, ^3J = 7.2, ^3J = 5.7, ^4J = 1.3 Hz, 1 H, H_j), 6.82 (ddd, ^3J = 7.2, ^3J = 5.7, ^4J = 1.3 Hz, 1 H, H_g), 2.33 (s, 3 H, NCCH_3), 2.32 (s, 3 H, NCCH_3) ppm. HRESI-MS: m/z = 563.04774 [M^+] (calcd. for $RuC_{38}H_{26}N_5O_5S^+$: m/z = 563.04796). $RuC_{30}H_{24}N_5OSPF_6$ (748.64) + 0.5CH_2Cl_2 (84.93): calcd. C 46.31, H 3.19, N 8.85; found C 46.51, H 3.44, N 8.82.

$[Ru(bpy)(deeb)(ppy)](PF_6)$ (1c): A suspension of **1b** (210 mg, 0.329 mmol) and deeb (98 mg, 0.33 mmol) in absolute EtOH (80 mL) was heated at reflux for 2 h. Solvent was removed from the purple solution, and then purified by column chromatography (SiO_2: CH_2Cl_2/MeCN, 9:1, 14.5 × 4 cm; R_f = 0.74) to yield 218 mg (77.4%) of the product as a purple solid. ^{1}H NMR (CD_3OD): δ = 9.09 (dd, ^4J = 1 Hz, 1 H, H_t), 8.98 (dd, ^4J = 1 Hz, 1 H, H_s), 8.49 (dd, ^3J = 8.0 Hz, 1 H, H_m), 8.49 (d, ^3J = 8.0 Hz, 1 H, H_l), 8.37 (dd, ^3J = 6.0, ^5J = 0.6 Hz, 1 H, H_q), 8.12 (dd, ^3J = 5.6, ^5J = 0.7 Hz, 1 H, H_v), 8.08 (d, ^3J = 8.1 Hz, 1 H, H_e), 7.98 (dd, ^3J = 5.6, ^4J = 1.6 Hz, 1 H, H_u), 7.92–7.86 (m, 3 H, $H_{d,k,n}$), 7.78 (ddd, ^3J = 5.7, ^4J = 1.4, ^5J = 0.7 Hz, 1 H, H_i), 7.75–7.70 (m, 2 H, $H_{f,r}$), 7.66 (ddd, ^3J = 5.7, ^4J = 1.4, ^5J = 0.7 Hz, 1 H, H_p), 7.50 (ddd, ^3J = 5.7, ^4J = 1.5, ^5J = 0.7 Hz, 1 H, H_h), 7.31 (ddd, ^3J = 7.2, 5.7, ^4J = 1.3 Hz, 1 H, H_j), 7.27 (ddd, ^3J = 7.2, 5.7, ^4J = 1.2 Hz, 1 H, H_o), 6.96–6.91 (m, 2 H, $H_{g,c}$), 6.84 (dt, ^3J = 7.4, ^4J = 1.3 Hz, 1 H, H_b), 6.39 (dd, ^3J = 7.4, ^4J = 0.8 Hz, 1 H, H_a), 4.49 (q, ^3J = 7.1 Hz, 2 H, -CH_2-), 4.46 (q, ^3J = 7.1 Hz, 2 H, -CH_2-), 1.45 (t, ^3J = 7.1 Hz, 3 H, -CH_3), 1.42 (t, ^3J = 7.1 Hz, 3 H, -CH_3) ppm. ^{19}F NMR (CD_3OD): δ = –75.0 (d, ^1J = 707.5 Hz) ppm. MS (ESI): m/z = 712.4 [M^+] (calcd. for $[RuC_{37}H_{32}N_5O_4]^+$: m/z = 712.1). $RuC_{37}H_{32}N_5O_4PF_6$ (856.71): calcd. C 51.87, H 3.76, N 8.17; found C 51.77, H 3.81, N 8.04.

$[Ru(bpy)(deeb)(ppy\text{-}F_2)](PF_6)$ (2c): A suspension of **2b** (175 mg, 0.259 mmol) and deeb (78 mg, 0.26 mmol) in absolute EtOH (80 mL) was heated at reflux for 2 h. Solvent was removed from the purple solution, and then purified by successive column chromatographic steps [1. SiO_2: CH_2Cl_2/MeCN, 9:1, 14.5 × 4 cm; R_f =

0.70; 2. SiO_2: $CHCl_3$/MeOH, 9:1; R_f = 0.56] to yield 143 mg (61.8%) of the product as a purple solid. ^{1}H NMR (CD_3OD): δ = 9.08 (d, ^4J = 0.9 Hz, 1 H, H_t), 8.98 (d, ^4J = 1.2 Hz, 1 H, H_s), 8.55 (d, ^3J = 8.1 Hz, 2 H, $H_{l,m}$), 8.33 (s, ^3J = 6.0 Hz, 2 H, $H_{e,q}$), 8.09 (d, ^3J = 5.7 Hz, 1 H, H_v), 8.01–7.93 (m, 3 H, $H_{k,n,u}$), 7.81–7.74 (m, 3 H, $H_{f,i,r}$), 7.65 (ddd, ^3J = 5.7, ^4J = 1.3, ^5J = 0.6 Hz, 1 H, H_p), 7.59 (ddd, ^3J = 5.7, ^4J = 1.5, ^5J = 0.7 Hz, 1 H, H_h), 7.37 (ddd, ^3J = 7.4, 5.7, ^4J = 1.3 Hz, 1 H, H_j), 7.31 (ddd, ^3J = 7.4, 5.7, ^4J = 1.3 Hz, 1 H, H_o), 6.99 (ddd, ^3J = 7.2, 5.7, ^4J = 1.2 Hz, 1 H, H_g), 6.42 (ddd, ^3J = 12.9, 9.2, ^4J = 2.4 Hz, 1 H, H_g), 5.88 (dd, ^3J = 8.2, ^4J = 2.4 Hz, 1 H, H_a), 4.50 (q, ^3J = 7.1 Hz, 2 H, -CH_2-), 4.47 (q, ^3J = 7.1 Hz, 2 H, -CH_2-), 1.45 (t, ^3J = 7.1 Hz, 3 H, -CH_3), 1.43 (t, ^3J = 7.1 Hz, 3 H, -CH_3) ppm. ^{19}F NMR (CD_3OD): δ = –75.0 (d, ^1J = 707.5 Hz, 6 F), –111.0 (m, 1 F), –111.8 (m, 1 F) ppm. ^{31}P NMR: δ = –144 (sept, ^1J = 707 Hz, 1 P) ppm. MS (ESI): m/z = 748.3 [M^+] (calcd. for $[RuC_{37}H_{30}N_5O_4F_2]^+$: m/z = 748.1). $RuC_{37}H_{30}N_5O_4PF_8$ (892.70): calcd. C 49.78, H 3.39, N 7.85; found C 50.10, H 3.60, N 7.42.

[Ru(bpy)(deeb)(ppy4thio)](PF$_6$) (3c): A suspension of **1b** (225 mg, 0.300 mmol) and deeb (91 mg, 0.30 mmol) in absolute EtOH (600 mL) was heated at reflux for 3 h. Solvent was removed from the red/brown solution, and then purified by column chromatography [SiO_2: MeCN] but could not be separated from residual deeb. The mixture was used without further purification in the following step.

[Ru(bpy)(dcbpy)(ppy)](PF$_6$) (1d): A DMF/H_2O/NEt_3 solution (3:1:1 *v*:*v*:*v*; 25 mL) containing **1c** (273 mg, 0.319 mmol) was heated at reflux for 16 h. Subsequent removal of solvent under reduced pressure left a purple solid that was purified by column chromatography [SiO_2: MeOH/$CHCl_3$, 1:1; 4 × 20 cm; R_f = 0.40]. Solvent was removed in vacuo and the product sonicated in a 1:1 hexane/Et_2O solution and filtered to afford 40 mg (16%) of the product as a dark purple solid. ^{1}H NMR (CD_3OD): δ = 9.00 (s, 1 H, H_t), 8.92 (d, ^4J = 1.2 Hz, 1 H, H_s), 8.46–8.42 (m, 2 H, $H_{l,m}$), 8.12 (dd, ^3J = 5.8, ^5J = 0.6 Hz, 1 H, H_q), 8.05 (d, ^3J = 8.1 Hz, 1 H, H_e), 7.89–7.79 (m, 6 H, $H_{d,i,k,n,u,v}$), 7.71 (ddd, ^3J = 5.8, ^4J = 1.4, ^5J = 0.7 Hz, 1 H, H_p), 7.68 (ddd, ^3J = 8.4, 7.4, ^4J = 1.6 Hz, 1 H, H_f), 7.58 (dd, ^3J = 5.8, ^5J = 1.7 Hz, 1 H, H_r), 7.55 (ddd, ^3J = 5.7, ^4J = 1.5, ^5J = 0.7 Hz, 1 H, H_h), 7.27–7.23 (m, 2 H, $H_{j,o}$), 6.93 (ddd, ^3J = 7.2, 5.7, ^4J = 1.3 Hz, 1 H, H_g), 6.89 (ddd, ^3J = 8.0, 7.4, ^4J = 1.4 Hz, 1 H, H_c), 6.81 (dt, ^3J = 7.3, ^4J = 1.3 Hz, 1 H, H_b), 6.42 (dd, ^3J = 7.4, ^4J = 0.9 Hz, 1 H, H_a) ppm. HRMS (ESI): m/z = 656.087565 [M^+] (calcd. for $[RuC_{33}H_{24}N_5O_4]^+$: m/z = 656.087527). $RuC_{33}H_{24}N_5O_4PF_6$ (800.60)/$RuC_{33}H_{23}N_5O_4$ (1:1) (654.63) + 5H_2O (18.01): calcd. C 51.30, H 3.72, N 9.06; found C 51.22, H 4.04, N 8.76.

[Ru(bpy)(dcbpy)(ppy-F$_2$)](PF$_6$) (2d): A DMF/H_2O/NEt_3 solution (3:1:1 *v*:*v*:*v*; 25 mL) containing **2c** (105 mg, 0.118 mmol) was heated at reflux for 16 h. Subsequent removal of solvent under reduced pressure afforded a purple solid that was purified by column chromatography [SiO_2: MeOH/$CHCl_3$, 1:1; silica plug]. The resultant solid was basified with an aqueous NaOH solution until dissolved, and then drawn out of solution with a 0.2 M solution of $HPF_{6\ (aq)}$. The solid was filtered and washed with H_2O, diethyl ether and hexanes to afford 70 mg (71%) of the product as a dark purple solid. ^{1}H NMR (CD_3OD): δ = 9.08 (s, 1 H, H_t), 9.00 (d, ^4J = 1.2 Hz, 1 H, H_s), 8.51 (d, 2 H, $H_{l,m}$), 8.31 (d, ^3J = 8.5 Hz, 1 H, H_e), 8.23 (d, ^3J = 5.9 Hz, 1 H, H_q), 7.99 (d, ^3J = 5.6 Hz, 1 H, H_v), 7.94–7.90 (m, 3 H, $H_{k,n,u}$), 7.76–7.72 (m, 3 H, $H_{f,i,r}$), 7.67 (ddd, ^3J = 5.6, ^4J = 1.4, ^5J = 0.7 Hz, 1 H, H_p), 7.61 (ddd, ^3J = 5.7, ^4J = 1.5, ^5J = 0.7 Hz, 1 H, H_h), 7.34 (ddd, ^3J = 7.4, 5.7, ^4J = 1.3 Hz, 1 H, H_j), 7.31 (ddd, ^3J = 7.4, 5.7, ^4J = 1.3 Hz, 1 H, H_o), 6.98 (ddd, ^3J = 7.2, 5.7, ^4J = 1.3 Hz, 1 H, H_g), 6.39 (ddd, $^3J_{HF}$ = 12.9, 9.2, ^4J = 2.4 Hz, 1 H, H_c), 5.89 (ddd, $^3J_{HF}$ = 8.3, ^4J = 2.4 Hz, 1 H, H_a) ppm. ^{19}F NMR (CD_3OD): δ = –75.0 (d, ^1J = 707.5 Hz, 6 F), –111.1 (m, 1 F), –112.1 (q, ^3J = 9.2 Hz, 1 F) ppm. ^{31}P NMR: δ = –144 (sept, ^1J = 707.5 Hz, 1P). HRMS (ESI): m/z = 692.06852 [M^+] (calcd. for $[RuC_{33}H_{22}N_5O_4F_2]^+$: m/z = 692.068683). $RuC_{33}H_{22}N_5O_4PF_8$ (836.59)/$RuC_{33}H_{21}N_5O_4F_2$ (1:3) (690.61) + 4H_2O (18.01): calcd. C 53.19, H 3.15, N 9.40; found C 53.47, H 3.41, N 9.25.

[Ru(bpy)(dcbpy)(ppy4thio)](PF$_6$) (3d): A DMF/H_2O/NEt_3 solution (3:1:1 *v*:*v*:*v*; 25 mL) containing **3c** (247 mg, 0.300 mmol) was heated at reflux for 16 h. Subsequent removal of solvent under reduced pressure afforded a dark red solid that was purified by successive chromatographic steps [1. SiO_2: MeOH/$CHCl_3$, 1:1; R_f = 0.38; 2. Sephadex: MeOH]. After the solvent was removed under reduced pressure, the resultant solid was washed with MeCN and sonicated to yield black microcrystals (40 mg, 17%). H^1 NMR (CD_3OD): δ = 9.79 (s, 1 H, H_y), 9.03 (s, 1 H, H_t), 8.95 (d, ^4J = 1.1 Hz, 1 H, H_s), 8.48 (d, ^3J = 4.5 Hz, 1 H, H_m), 8.46 (d, ^3J = 4.6 Hz, 1 H, H_l), 8.25–8.21 (m, 2 H, $H_{d,i}$), 8.15 (d, ^3J = 5.9 Hz, 1 H, H_q), 7.92–7.72 (m, 8 H, $H_{e,h,k,n,p,u,v,x}$), 7.64–7.59 (m, 2 H, $H_{f,r}$), 7.55 (d, ^3J = 4.0 Hz, 1 H, H_w), 7.32–7.25 (m, 2 H, $H_{j,o}$), 7.18 (dd, ^3J = 7.8, ^4J = 1.9 Hz, 1 H, H_b), 7.02 (ddd, ^3J = 7.2, ^3J = 5.8, ^4J = 1.2 Hz, 1 H, H_g), 6.59 (d, ^3J = 7.8 Hz, 1 H, H_a) ppm. ESI-MS: m/z = 766.1 [M^+] (calcd. for $RuC_{38}H_{26}N_5O_5S^+$: m/z = 766.1). $RuC_{38}H_{26}N_5O_5SPF_6$ (910.74)/$RuC_{38}H_{25}N_5O_5S$ (1:1) (764.77) + 8H_2O (18.01): calcd. C 50.16, H 3.71, N 7.70; found C 49.66, H 3.92, N 7.33.

Physical Methods: 1D and 2D ^{1}H spectra were recorded at 400 MHz and ^{13}C spectra at 100 MHz on a Bruker AV 400 instrument at ambient temperature unless otherwise stated. Electrochemical measurements were performed under anaerobic conditions with a Princeton Applied Research VersaStat 3 potentiostat using dry solvents, Pt working and counter electrodes, a Ag pseudoreference electrode, and 0.1 M NBu_4BF_4 supporting electrolyte. Electronic spectroscopic data were collected on MeOH solutions using a Cary 5000 UV/Vis spectrophotometer (Varian). Steady-state emission spectra were obtained at room temperature using an Edinburgh Instruments FLS920 Spectrometer equipped with a Xe900 450W steady state xenon arc lamp, TMS300-X excitation monochromator, TMS300-M emission monochromator, Hamamatsu R2658P PMT detector and corrected for detector response. Lifetime measurements were obtained at room temperature using an Edinburgh Instruments FLS920 Spectrometer equipped with Fianium SC400 Super Continuum White Light Source, Hamamatsu R3809U-50 Multi Channel Plate detector and data were analyzed with Edinburgh Instruments F900 software. Curve fitting of the data was performed using a non-linear least-squares procedure in the F900 software.

Cell Fabrication: Photoanodes were prefabricated by Dyesol, Inc. (Australia) with screen-printable TiO_2 pastes (18-NRT and WER4-O, Dyesol™), and used without further post-treatment (i.e. $TiCl_4$) The active area of the TiO_2 electrode is 0.28 cm^2 with a thickness of 12 μm (18-NRT) and 3 μm (WER4-O) on fluorine-doped tin-oxide (FTO; TEC-15Ω). The electrodes were heated to 450 °C for 20 min under ambient atmosphere and allowed to cool to 80 °C before dipping into the dye solution. The anode was soaked overnight for 16 h in a dye solution with a concentration of ca. 0.2 mM in absolute EtOH. The stained films were rinsed copiously with absolute EtOH and dried. The cells were fabricated using Pt-coated counter-electrode (FTO TEC-15Ω) and sealed with a 30 μm Surlyn (Dupont) gasket by resistive heating. An acetonitrile based electrolyte solution (0.60 M butylmethylimidazolium iodide, 0.03 M I_2, 0.10 M guanidinium thiocyanate and 0.50 M *tert*-butylpyridine) was introduced to the void via vacuum backfilling through a hole in

the counter electrode. The hole was sealed with an aluminum-backed Bynel foil (Dyesol™).

Dye Characterization: The extent of dye-loading was measured by dipping TiO_2 into an absolute ethanol solution of each sensitizer. After 16 h of dipping the adsorbed dye was removed with a 0.05 M NaOH solution in methanol. The solution obtained was measured by UV/Vis and compared against a calibrated absorption curve of dye in the same solvent to obtain the amount of dye desorbed. All cells were measured under standard AM1.5 conditions. $E(S^+/S^*)$ calculated using $E(S^+/S^*) = E(S^+/S) - E^{(0-0)}$ where $E^{(0-0)}$ is obtained from the higher energy side of corrected emission band where the intensity is ca. 10% of the maximum.[29] Optical cross-section (σ in cm^2) is calculated from $\sigma(\lambda) = 1000\varepsilon(\lambda)/[N_A\log(e)]$ (N_A is Avogadro's number and e is Euler's number) and subsequently converted to nm^2.[63]

Cell Characterization: Photovoltaic measurements were recorded with a Newport Oriel solar simulator (Model 9225A1) equipped with a class A 450-W xenon light source powered by a Newport power supply (Model 69907). The light output (area: 5×5 cm) was calibrated to AM 1.5 using a Newport Oriel correction filter to reduce the spectral mismatch in the region of 350–700 nm to less than 1.5%. The power output of the lamp was measured to 1 Sun (100 mW cm^{-2}) using a certified Si reference cell. The current–voltage characteristic of each cell was obtained by applying an external potential bias to the cell and measuring the generated photocurrent with a Keithley digital source meter (Model 2400). IPCE measurements were performed at PV Measurements Inc. (USA).

DFT Calculations: Density functional theory (DFT) calculations were carried out using B3LYP [Becke's three-parameter exchange functional (B3)[64] and the Lee–Yang–Parr correlation functional (LYP)[65]] and the LanL2DZ basis set. All geometries were fully optimized in the ground states (closed-shell singlet S_0). Time-dependent density functional theory (TD-DFT) calculations were performed with IEFPCM solvation model (MeCN) using a spin-restricted formalism to examine low-energy excitations at the ground-state geometry. All calculations were carried out with the Gaussian 03W software package.[66]

Supporting Information (see footnote on the first page of this article): ^{1}H NMR and UV/Vis spectra, cyclic voltammograms for **1a**–**1d**, and IPCE data for **1d**–**3d**.

Acknowledgments

This work was financially supported by the Canadian Natural Science and Engineering Research Council (NSERC), Canada Research Chairs, Canada Foundation for Innovation, Alberta Ingenuity and The Institute for Sustainable Energy, Environment & Economy. P. G. B. acknowledges Alberta Innovates – Technology Futures formerly Alberta Ingenuity and NSERC for financial support. K. D. T. acknowledges NSERC and the University of Calgary Nanotech Recruitment Centre for financial support.

[1] D. Shi, N. Pootrakulchote, R. Li, J. Guo, Y. Wang, S. M. Zakeeruddin, M. Grätzel, P. Wang, *J. Phys. Chem. C* **2008**, *112*, 17046–17050.
[2] B. Azzopardi, J. Mutale, *Renewable Sustainable Energy Rev.* **2010**, *14*, 1130–1134.
[3] H. Greijer, L. Karlson, S.-E. Lindquist, H. Anders, *Renewable Energy* **2001**, *23*, 27–39.
[4] A. F. Sherwani, J. A. Usmani, Varun, *Renewable Sustainable Energy Rev.* **2010**, *14*, 540–544.
[5] M. A. Green, K. Emery, Y. Hishikawa, W. Warta, *Prog. Photovoltaics* **2010**, *18*, 144–150.
[6] Q. Yu, Y. Wang, Z. Yi, N. Zu, J. Zhang, M. Zhang, P. Wang, *ACS Nano* **2010**, *4*, 6032–6038.
[7] G. K. Mor, O. K. Varghese, M. Paulose, K. Shankar, C. A. Grimes, *Sol. Energy Mater. Sol. Cells* **2006**, *90*, 2011–2075.
[8] M. Law, L. E. Greene, J. C. Johnson, R. Saykally, P. Yang, *Nat. Mater.* **2005**, *4*, 455–459.
[9] B. C. O'Regan, J. R. Durrant, *Acc. Chem. Res.* **2009**, *42*, 1799–1808.
[10] A. M. Spokoyny, T. C. Li, O. K. Farha, C. W. Machan, C. She, C. L. Stern, T. J. Marks, J. T. Hupp, C. A. Mirkin, *Angew. Chem. Int. Ed.* **2010**, *49*, 5339–5343.
[11] T. C. Li, A. M. Spokoyny, C. She, O. K. Farha, C. A. Mirkin, T. J. Marks, J. T. Hupp, *J. Am. Chem. Soc.* **2010**, *132*, 4580–4582.
[12] X. Liu, W. Zhang, S. Uchida, L. Cai, B. Liu, S. Ramakrishna, *Adv. Mater.* **2010**, *22*, E150–E155.
[13] M. Graetzel, *Inorg. Chem.* **2005**, *44*, 6841–6851.
[14] N. Robertson, *Angew. Chem.* **2008**, *120*, 1028; *Angew. Chem. Int. Ed.* **2008**, *47*, 1012–1014.
[15] N. Robertson, *Angew. Chem.* **2006**, *118*, 2398; *Angew. Chem. Int. Ed.* **2006**, *45*, 2338–2345.
[16] B. O'Regan, M. Grätzel, *Nature* **1991**, *353*, 737–740.
[17] M. K. Nazeeruddin, A. Kay, I. Rodicio, R. Humphry-Baker, E. Mueller, P. Liska, N. Vlachopoulos, M. Grätzel, *J. Am. Chem. Soc.* **1993**, *115*, 6382–6390.
[18] M. K. Nazeeruddin, S. M. Zakeeruddin, R. Humphry-Baker, M. Jirousek, P. Liska, N. Vlachopoulos, V. Shklover, C.-H. Fischer, M. Grätzel, *Inorg. Chem.* **1999**, *38*, 6298–6305.
[19] M. K. Nazeeruddin, P. Pechy, T. Renouard, S. M. Zakeeruddin, R. Humphry-Baker, P. Comte, P. Liska, L. Cevey, E. Costa, V. Shklover, L. Spiccia, G. B. Deacon, C. A. Bignozzi, M. Grätzel, *J. Am. Chem. Soc.* **2001**, *123*, 1613–1624.
[20] P. Wang, S. M. Zakeeruddin, J. E. Moser, R. Humphry-Baker, P. Comte, V. Aranyos, A. Hagfeldt, M. K. Nazeeruddin, M. Grätzel, *Adv. Mater.* **2004**, *16*, 1806–1811.
[21] M. K. Nazeeruddin, T. Bessho, L. Cevey, S. Ito, C. Klein, F. De Angelis, S. Fantacci, P. Comte, P. Liska, H. Imai, M. Grätzel, *J. Photochem. A* **2007**, *185*, 331–337.
[22] F. Gao, Y. Wang, D. Shi, J. Zhang, M. K. Wang, X. Y. Jing, R. Humphry-Baker, P. Wang, S. M. Zakeeruddin, M. Grätzel, *J. Am. Chem. Soc.* **2008**, *130*, 10720–10728.
[23] F. Gao, Y. Wang, J. Zhang, D. Shi, M. K. Wang, R. Humphry-Baker, P. Wang, S. M. Zakeeruddin, M. Grätzel, *Chem. Commun.* **2008**, 2635–2637.
[24] Y. Cao, Y. Bai, Q. Yu, Y. Cheng, S. Liu, D. Shi, F. Gao, P. Wang, *J. Phys. Chem. C* **2009**, *113*, 6290–6297.
[25] F. Gao, Y. Cheng, Q. Yu, S. Liu, D. Shi, Y. Li, P. Wang, *Inorg. Chem.* **2009**, *48*, 2664–2669.
[26] Q. Yu, S. Liu, M. Zhang, N. Cai, Y. Wang, P. Wang, *J. Phys. Chem. C* **2009**, *113*, 14559–14566.
[27] W. Zeng, Y. Cao, Y. Bai, Y. Wang, Y. Shi, M. Zhang, F. Wang, C. Pan, P. Wang, *Chem. Mater.* **2010**, *22*, 1915–1925.
[28] T. Bessho, S. Zakeeruddin, C. Y. Yeh, E. G. Diau, M. Grätzel, *Angew. Chem. Int. Ed.* **2010**, *49*, 6646–6649.
[29] T. Bessho, E. Yoneda, J.-H. Yum, M. Guglielmi, I. Tavernelli, H. Imai, U. Rothlisberger, M. K. Nazeeruddin, M. Grätzel, *J. Am. Chem. Soc.* **2009**, *131*, 5930–5934.
[30] K.-L. Wu, H.-C. Hsu, K. Chen, Y. Chi, M.-W. Chung, W.-H. Liu, P.-T. Chou, *Chem. Commun.* **2010**, *46*, 5124–5126.
[31] M. Beley, J. P. Collin, J. P. Sauvage, *Inorg. Chem.* **1993**, *32*, 4539–4543.
[32] J. P. Collin, S. Guillerez, J. P. Sauvage, F. Barigelletti, L. De Cola, L. Flamigni, V. Balzani, *Inorg. Chem.* **1991**, *30*, 4230–4238.
[33] E. C. Constable, C. E. Housecroft, *Polyhedron* **1990**, *9*, 1939–1947.
[34] E. C. Constable, J. M. Holmes, *J. Organomet. Chem.* **1986**, *301*, 203–208.

[35] S. Fernandez, M. Pfeffer, V. Ritleng, C. Sirlin, *Organometallics* **1999**, *18*, 2390–2394.
[36] M. Jager, A. Smeigh, F. Lombeck, H. Gorls, J.-P. Collin, J.-P. Sauvage, L. Hammarström, O. Johansson, *Inorg. Chem.* **2010**, *49*, 374–376.
[37] S. Ott, M. Borgstrom, L. Hammarström, O. Johansson, *Dalton Trans.* **2006**, 1434–1443.
[38] C.-J. Yao, L.-Z. Sui, H.-Y. Xie, W.-J. Xiao, Y.-W. Zhong, J. Yao, *Inorg. Chem.* **2010**, *49*, 8347–8350.
[39] S. H. Wadman, J. M. Kroon, K. Bakker, M. Lutz, A. L. Spek, G. P. M. van Klink, G. van Koten, *Chem. Commun.* **2007**, 1907–1909.
[40] P. G. Bomben, K. C. D. Robson, P. A. Sedach, C. P. Berlinguette, *Inorg. Chem.* **2009**, *48*, 9631–9643.
[41] S. H. Wadman, J. M. Kroon, K. Bakker, R. W. A. Havenith, G. P. M. van Klink, G. van Koten, *Organometallics* **2010**, *29*, 1569–1579.
[42] P. G. Bomben, B. D. Koivisto, C. P. Berlinguette, *Inorg. Chem.* **2010**, *49*, 4960–4971.
[43] S. Ardo, G. J. Meyer, *Chem. Soc. Rev.* **2009**, *38*, 115–164.
[44] S. M. Zakeeruddin, M. Nazeeruddin, R. Humphry-Baker, P. Pechy, P. Quagliotto, C. Barolo, G. Viscardi, M. Grätzel, *Langmuir* **2002**, *18*, 952–954.
[45] A. D. Ryabov, V. S. Sukharev, L. Alexandrova, R. Le Lagadec, M. Pfeffer, *Inorg. Chem.* **2001**, *40*, 6529–6532.
[46] N. G. Connelly, W. E. Geiger, *Chem. Rev.* **1996**, *96*, 877–910.
[47] E. C. Constable, T. A. Leese, *J. Organomet. Chem.* **1987**, *335*, 293–299.
[48] M. Grätzel, *Nature* **2001**, *414*, 338–344.
[49] S. H. Wadman, M. Lutz, D. M. Tooke, A. L. Spek, F. Hartl, R. W. A. Havenith, G. P. M. van Klink, G. van Koten, *Inorg. Chem.* **2009**, *48*, 1887–1900.
[50] L. Karki, H. P. Lu, J. T. Hupp, *J. Phys. Chem.* **1996**, *100*, 15637–15639.
[51] B. S. Brunschwig, C. Creutz, N. Sutin, *Coord. Chem. Rev.* **1998**, *177*, 61–79.
[52] E. J. J. Groenen, P. N. T. Van Velzen, *Mol. Phys.* **1977**, *33*, 933–942.
[53] G. Boschloo, A. Hagfeldt, *Acc. Chem. Res.* **2009**, *42*, 1819–1826.
[54] T. W. Hamann, R. A. Jensen, A. B. F. Martinson, H. Van Ryswyk, J. T. Hupp, *Energy Environ. Sci.* **2008**, *1*, 66–78.
[55] S. Wenger, P.-A.Bouit, Q. Chen, J. Teuscher, D. Di Censo, R. Humphry-Baker, J.-E. Moser, J. L. Delgado, N. Martin, S. M. Zakeeruddin, M. Grätzel, *J. Am. Chem. Soc.* **2010**, *132*, 5164–5169.
[56] These values are obtained in the gas-phase, and may not accurately reflect the dipole of the dyes bound to the TiO2 surface.
[57] F. De Angelis, S. Fantacci, A. Selloni, M. Grätzel, K. Nazeeruddin Mohammed, *Nano Lett.* **2007**, *7*, 3189–3195.
[58] S. Ruehle, M. Greenshtein, S. G. Chen, A. Merson, H. Pizem, C. S. Sukenik, D. Cahen, A. Zaban, *J. Phys. Chem. B* **2005**, *109*, 18907–18913.
[59] S. Nakade, T. Kanzaki, W. Kubo, T. Kitamura, Y. Wada, S. Yanagida, *J. Phys. Chem. B* **2005**, *109*, 3480–3487.
[60] M. J. Palmer, J. A. Kenny, T. Walsgrove, A. M. Kawamoto, M. Wills, *J. Chem. Soc. Perkin Trans. 1* **2002**, 416–427.
[61] P. G. Hoertz, A. Staniszewski, A. Marton, G. T. Higgins, C. D. Incarvito, A. L. Rheingold, G. J. Meyer, *J. Am. Chem. Soc.* **2006**, *128*, 8234–8245.
[62] A. D. Ryabov, R. Le Lagadec, H. Estevez, R. A. Toscano, S. Hernandez, L. Alexandrova, V. S. Kurova, A. Fischer, C. Sirlin, M. Pfeffer, *Inorg. Chem.* **2005**, *44*, 1626–1634.
[63] N. Gotsche, H. Ulbricht, M. Arndt, *Laser Phys.* **2007**, *17*, 583–589.
[64] A. D. Becke, *Phys. Rev. A: Gen. Phys.* **1988**, *38*, 3098–3100.
[65] C. Lee, W. Yang, R. G. Parr, *Phys. Rev. B: Condens. Matter* **1988**, *37*, 785–789.
[66] M. J. Frisch, G. W. Trucks, H. B. Schlegel, G. E. Scuseria, M. A. Robb, J. R. Cheeseman, J. A. Montgomery, Jr., T. Vreven, K. N. Kudin, J. C. Burant, J. M. Millam, S. S. Iyengar, J. Tomasi, V. Barone, B. Mennucci, M. Cossi, G. Scalmani, N. Rega, G. A. Petersson, H. Nakatsuji, M. Hada, M. Ehara, K. Toyota, R. Fukuda, J. Hasegawa, M. Ishida, T. Nakajima, Y. Honda, O. Kitao, H. Nakai, M. Klene, X. Li, J. E. Knox, H. P. Hratchian, J. B. Cross, V. Bakken, C. Adamo, J. Jaramillo, R. Gomperts, R. E. Stratmann, O. Yazyev, A. J. Austin, R. Cammi, C. Pomelli, J. W. Ochterski, P. Y. Ayala, K. Morokuma, G. A. Voth, P. Salvador, J. J. Dannenberg, V. G. Zakrzewski, S. Dapprich, A. D. Daniels, M. C. Strain, O. Farkas, D. K. Malick, A. D. Rabuck, K. Raghavachari, J. B. Foresman, J. V. Ortiz, Q. Cui, A. G. Baboul, S. Clifford, J. Cioslowski, B. B. Stefanov, G. Liu, A. Liashenko, P. Piskorz, I. Komaromi, R. L. Martin, D. J. Fox, T. Keith, M. A. Al-Laham, C. Y. Peng, A. Nanayakkara, M. Challacombe, P. M. W. Gill, B. Johnson, W. Chen, M. W. Wong, C. Gonzalez, J. A. Pople, *Gaussian 03*, rev. c.02, Gaussian Inc., Wallingford, CT, **2004**.

Received: December 22, 2010
Published Online: March 11, 2011

